RESEARCH ARTICLE

Macromolecular Chemistry and Physics
www.mcp-journal.de

Poly(oxanorbornene)-Based Polyzwitterions with Systematically Increasing Hydrophobicity: Synthesis, Physical Characterization, and Biological Properties

*Stefan Paschke, Franziska Marx, Vera Bleicher, Alice Eickenscheidt, and Karen Lienkamp**

Surfaces coated with polyzwitterions are known to resist protein adhesion and to be generally bio-inert. In recent reports, several polyzwitterionic coatings with carboxylate groups and intrinsic antimicrobial activity due to the pH-responsivity of that group are described, but the design rules to obtain such activity remain unclear. Therefore, in this work, a set of surface-attached polyzwitterions with carboxylate groups and varying alkyl residues is studied. The gradually increasing hydrophobicity of these surfaces (verified by contact angle and swellability measurements) has an impact on their biological properties. Hydrophilic surfaces (polyzwitterions bearing short alkyl residues) behave like "classical" polyzwitterions: they repel proteins and human cells and are non-toxic to bacteria. The more hydrophobic polyzwitterionic surfaces are protein-adhesive, cell-toxic, and can kill bacteria. This indicates that the hydrophobicity of polyzwitterionic surfaces needs to be balanced precisely to combine protein-repellency and antimicrobial activity in a single material.

1. Introduction

Mammalian cell membranes consist of phospholipids with highly hydrated, mostly zwitterionic head-groups. Proteins have a low tendency to attach to these overall charge-neutral membranes, so that the selective, receptor-mediated interactions of the membrane with other bioactive molecules remain undisturbed by unspecific protein adsorption. This concept was imitated in a number of investigations where polyzwitterions were surface-attached to create protein-repellent materials, for example, as polymer brushes or polymer networks.[1–7] These studies showed that at a sufficiently high coverage with polyzwitterions, protein adsorption was drastically reduced.[1–7] Materials with such properties have been termed as "non-fouling" or (more precisely) "protein-repellent". Protein adsorption on surfaces is often quantified by surface plasmon resonance spectroscopy (SPR), a method where surface plasmons are excited in a gold layer by laser light irradiation. Any kind of adsorption of matter on that layer is detected through a shift of the laser light absorption minimum, that is, a shift in the resonance conditions for the surface plasmons. Previous studies have shown that surfaces with "ultra-low fouling" tendency adsorb proteins by less than 5 ng cm^{-2}.[7–12]

The dominating physical factors that cause the protein-repellency of polyzwitterionic surfaces and other highly hydrophilic non-fouling polymer materials are controversially discussed in the literature,[13] yet there seems to be an overall agreement that they are the sum of different thermodynamic contributions. First, due to their high charge density and dipole moment, polyzwitterions swell strongly in aqueous media, so that the free enthalpy of protein adhesion on these materials is low. Second, polyzwitterions do not disturb the hydrogen bonds near the material-water-interface, that is, the surfaces "look like water", and breaking this structure during protein adhesion would be enthalpically unfavorable.[14] Third, protein permeation of (already stretched) polymer chains that are part of a polymer brush architecture or a swollen network is enthalpically and entropically unfavorable.[13]

Most protein-repellent polyzwitterionic surfaces are non-adhesive for bacteria because protein adhesion is also the first step of bacterial adhesion.[9,15–17] Thus, polyzwitterions are considered as bio-inert. This is especially true for polyzwitterions containing pH-inert groups such as sulfonic acid groups and quaternary ammonium groups ("strong electrolyte" groups), but also for those containing pH-responsive carboxylic acid groups (a "weak electrolyte") in combination with quaternary ammonium

S. Paschke, F. Marx, V. Bleicher, A. Eickenscheidt, K. Lienkamp
Department of Microsystems Engineering (IMTEK)
University of Freiburg
Georges-Köhler-Allee 103, 79110 Freiburg, Germany
E-mail: karen.lienkamp@uni-saarland.de
S. Paschke, F. Marx, V. Bleicher, A. Eickenscheidt, K. Lienkamp
Freiburg Center for Interactive Materials and Bioinspired Technologies (FIT)
University of Freiburg
Georges-Köhler-Allee 105, 79110 Freiburg, Germany
K. Lienkamp
Department of Materials Science and Engineering
Saarland University
Campus, 66123 Saarbrücken, Germany

The ORCID identification number(s) for the author(s) of this article can be found under https://doi.org/10.1002/macp.202200334

DOI: 10.1002/macp.202200334

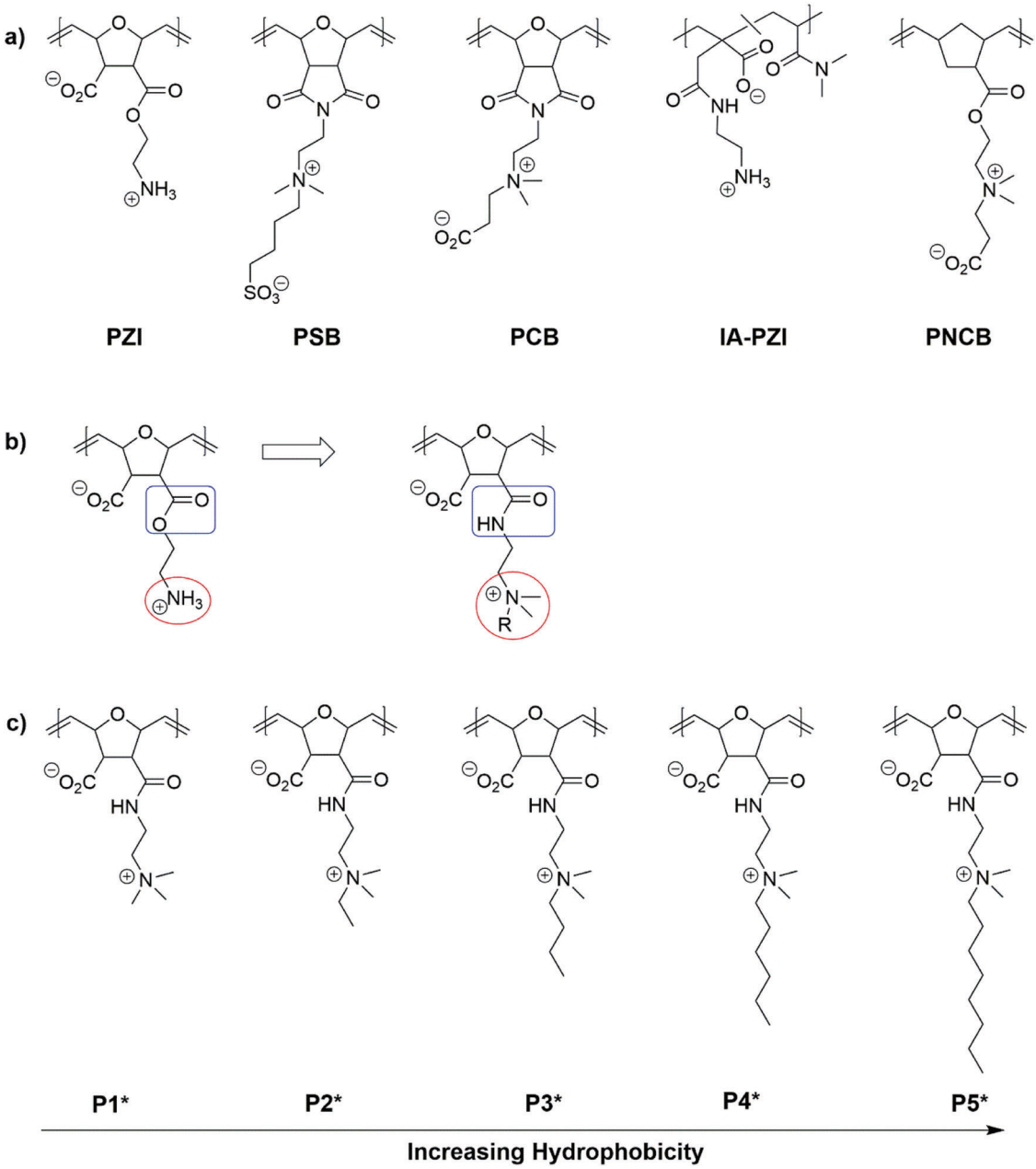

Figure 1. a) Chemical structures of the pH-responsive polyzwitterions PZI, PCB, IA-PZI, and PNCB, which were intrinsically antimicrobial, and the pH-inert polyzwitterion PSB.[20–23] b) Molecular design of the polyzwitterions reported in this work (right), and the parent structure PZI (left).[20] To increase the hydrolytic stability of the target polymers, the ester bonds of PZI were replaced by amide bonds, and the primary ammonium group was exchanged for quaternary ammonium groups with different alkyl residues. c) Chemical structure of the target polyzwitterions. Different alkyl residues from methyl to octyl were used to systematically increase the hydrophobicity of the structures.

groups. In this context, it was reported that poly(carboxybetaine) hydrogels, in contrast to most other known implant materials, do not induce an inflammatory response.[18,19] Our group recently published a study in which the physical properties and bioactivity of three surface-attached polyzwitterionic poly(oxanorbornene) networks were compared (**Figure 1**a): the poly(carboxyzwitterion) PZI containing primary ammonium groups together with carboxylate groups (both weak electrolytes), the poly(sulfobetaine) PSB with quaternary ammonium groups and sulfonate groups (both strong electrolytes), and the poly(carboxybetaine) PCB, with quaternary ammonium groups and carboxylate groups (mixed).[20,21] The poly(norbornene)-based poly(carboxybetaine) PNCB, a structural variant of PCB, was also recently reported,[22] as well as the poly(carboxyzwitterion) IA-PZI, the structural analog of PZI with a poly(itaconic acid) backbone.[23] When these polyzwitterions were surface-attached as networks, they showed the expected protein repellency.

Additionally, PZI, IA-PZI, PCB, and PNCB had intrinsic antimicrobial activity.[20–23] This was remarkable because antimicrobial activity and protein repellency are considered to be mutually exclusive: intrinsic activity against bacteria requires cationic charges, which also induce protein adsorption. To understand this contradiction, the pH-dependent surface zeta potential of these polyzwitterions was studied. In these studies, PSB had a negative zeta potential which was independent of the pH value over a large range, as expected for a polyzwitterion with two pH-inert functional groups. The other polymers showed a pH-dependent zeta potential which was increasingly positive at low pH-values. This was attributed to the protonation of the carboxylate groups of PZI, PCB, and IA-PZI and led to the hypothesis that the observed antimicrobial activity of these materials was caused by protonation in the presence of bacteria, which produce acidic metabolites. By this mechanism, the surfaces might become polycationic locally and near incoming bacteria only, which causes the observed antimicrobial activity. At the other surface sites, the material would stay polyzwitterionic and therefore protein-repellent.[20] Thus, the reported polyzwitterions are stimulus-responsive, with a switching point at a slightly acidic pH. The reversibility of this effect was confirmed by protein adhesion and release experiments using PNCB. While that material was protein-adhesive at low pH, an adsorbed protein layer was fully released when the pH value was switched back to neutral.[22]

Multi-component polymer systems that were designed for simultaneous protein repellency and antimicrobial activity have also been described in the literature. In most reports of such materials, the desired properties were not fully obtained, that is, either the obtained antimicrobial activity was reduced, or the level of protein repellency was compromised. Additionally, the preparation of many of those materials was complex.[24–27] Other systems, particularly the beautifully designed polyzwitterionic/polycationic surfaces reported by the Jiang group, which were pioneer works for the field of switchable antimicrobial surfaces, could be switched from a polycationic, adhesive state into a polyzwitterionic, protein-repellent state, yet the switching was either irreversible or needed harsh regeneration conditions.[15,16,28] Thus, in summary, the merit of the polyzwitterions PZI, PCB, and IA-PZI is that they are switchable between the antimicrobial and protein-repellent state by reversible protonation under mild conditions, and that they seem to be self-activating in the presence of metabolizing bacteria.

From the structures of these polymers, it follows that an overall polyzwitterionic nature and a carboxylate group are required for on-demand switchable surface properties. However, since there are also examples in the literature where poly(carboxybetaines) have been tested negatively for antimicrobial activity,[15,16,29,30] these cannot be the only requirements for antimicrobial activity in the protonated state. Upon further inspection of their structure, it becomes clear that two of the four antimicrobial polyzwitterions (PZI an IA-PZI, Figure 1a) bear structural similarities to previously reported antimicrobial polycations bearing hydrophobic groups, one with a poly(oxanorbornene) backbone, and one based on poly(itaconic acid).[31,32] Polycations of this type are known as "Synthetic Mimics of Antimicrobial Peptides" (SMAMPs) since they imitate the facial amphiphilicity of antimicrobial peptides (AMPs), with hydrophobic as well as cationic functional groups regularly distributed over the molecule. We assume that the SMAMP-like distribution of hydrophobicity, in addition to their hydrophilic, cationic groups and their carboxylate groups, is crucial for the antimicrobial activity of the polyzwitterions PZI, PCB, IA-PZI, and PNCB. This design principle needs to be confirmed by a model study with polyzwitterions of gradually increasing hydrophobicity, which is the purpose of this work.

2. Results and Discussion

2.1. Study Design

The aim of this study was to confirm the hypothesis that pH-responsive polyzwitterions become antimicrobially active in the protonated state if they are also substantially hydrophobic. Additionally, we wanted to investigate how such an increase in hydrophobicity affects other physical and biological properties quantitatively, notably protein repellency and cell compatibility. Thus, we designed a series of polyzwitterions with systematically increasing hydrophobicity. The generic structure of these target polymers is shown in Figure 1b, together with the parent structure PZI from which it was derived. The target structure is a fully alkylated version of PZI, with two methyl substituents and another alkyl substituent R with varying lengths (R = methyl, ethyl, butyl, hexyl, and octyl, Figure 1c). An amide bond was chosen to connect the hydrophobic/cationic side chains to the polymer backbone as it has higher stability against hydrolysis than an ester group. The quaternary ammonium groups instead of the primary ammonium groups as in PZI should further enhance the stability of the molecule.

As zwitterionic monomers are notoriously difficult to handle and to polymerize, we adapted a procedure by Colak and Tew and obtained the target structures via their polycationic analogs.[10] In short, the cationic monomers were synthesized by alkylation of a common precursor, and then polymerized by ring-opening metathesis polymerization (ROMP). These polycations were then surface-attached as networks and hydrolyzed to yield the desired polyzwitterionic networks. Afterwards, the physical and biological properties were analyzed to derive structure-property relationships.

2.2. Synthesis

The target poly(zwitterionic) networks were synthesized via their polycationic precursors, as previously reported for similar structures.[10] First, the cationic monomers M1–M5 with different alkyl residues on the nitrogen atom were synthesized from monomer precursor A (**Figure 2**a) using different alkylating agents. The products, monomers M1 to M5, precipitated from the reaction solution and were recovered by filtration. Their chemical structure was confirmed by ^{1}H–NMR spectroscopy and mass spectrometry as shown in Figures S1–S4, Supporting Information. Monomer M1 was copolymerized with 20 mol-% of the comonomer Diazo-M (Figure 2b, previously reported in the literature)[33] via ring-opening metathesis polymerization using a Grubbs 3rd generation catalyst, yielding the cationic copolymer P(1-co-Diazo$_{20}$) (Figure 2b).

M2–M5 were homopolymerized using the same catalyst. The polycations were characterized by ^{1}H–NMR–spectroscopy (Figures S5 and S6, Supporting Information) and gel-permeation

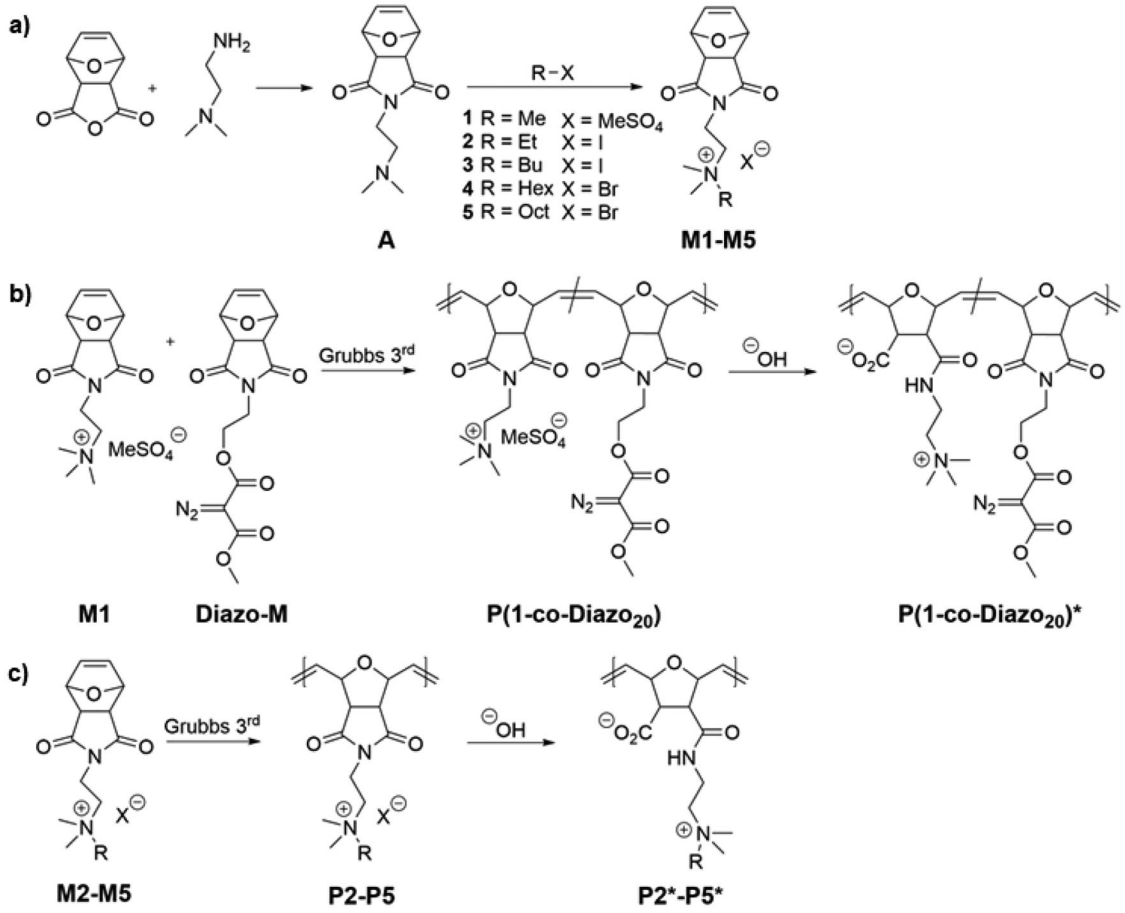

Figure 2. Synthesis of the cationic precursor polymers and the targeted polyzwitterions. a) The monomer precursor A was reacted with different alkylating agents to yield the monomers M1 to M5. b) M1 was copolymerized with the crosslinker monomer Diazo-M via ROMP using Grubbs 3rd generation catalyst, yielding copolymer P(1-co-Diazo$_{20}$). c) The cationic monomers M2–M5 were homopolymerized by ROMP to obtain polymers P2 to P5. After their transformation into surface-attached polymer networks, P(1-co-Diazo$_{20}$) and P2 to P5 were hydrolyzed, yielding the polyzwitterionic networks P(1-co-Diazo$_{20}$)* and P2* to P5*.

Table 1. Molar mass of the polycations determined by GPC (TFE, 0.05 M potassium trifluoroacetate, PMMA-standard, 40 °C, PFG-column).

Polymer	M_n [g mol^{-1}]	M_w [g mol^{-1}]	Mw/Mn
P(1-co-Diazo$_{20}$)	54 000	77 000	1.44
P2	40 000	48 000	1.20
P3	40 000	47 000	1.17
P4	44 000	57 000	1.30
P5	39 000	46 000	1.17

chromatography (GPC, **Table 1**, Figure S7, Supporting Information). The results of the GPC analysis (in trifluoroethanol, TFE) are summarized in Table 1, the corresponding elugrams are shown in Figure S7, Supporting Information. All the polymers had a number-average molar mass M_n > 30 000 g mol^{-1} and narrow molecular weight distributions. These molar masses are probably an overestimation, since the GPC calibration standard used was poly(methyl methacrylates) (PMMA), while the structures synthesized had the more rigid poly(oxanorbornene) backbone, and thus a larger hydrodynamic radius than the more compact PMMA polymers. However, the absolute number of M_n is of little relevance in this context, as long as it is sufficient to produce polymer solutions with suitable viscosity for the following spin-coating process.

2.3. Network Formation, Hydrolysis, and Physical Characterization

To obtain the polyzwitterionic networks, the cationic polymers were spin-coated onto silicon wafers, crosslinked by UV irradiation, and then hydrolyzed under basic conditions. In order to obtain covalent bonds between the silicon substrate and the polymer chains, the wafers were pre-functionalized with benzophenone groups as previously reported.[20] To that end, polymer P(1-co-Diazo$_{20}$) with the internal diazo crosslinker was dissolved in TFE and spin-coated onto these substrates. Irradiation with UV light simultaneously triggered the crosslinking of the polymer chains through the diazo groups, and the covalent attachment to the wafer via the benzophenone groups (**Figure 3**a).[33] For

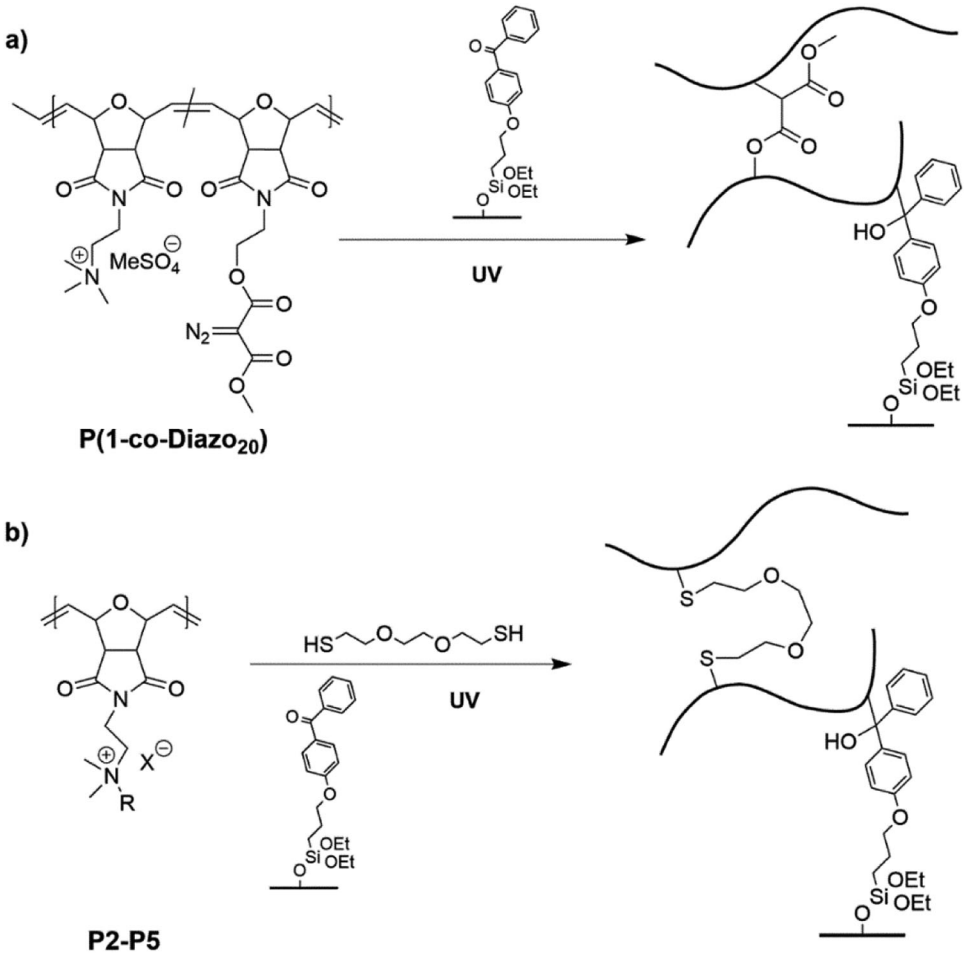

Figure 3. UV-activated formation of surface-attached polymer networks: a) P(1-co-Diazo$_{20}$) containing an internal crosslinker was crosslinked and surface-attached via two simultaneous C,H-insertion reactions; b) P2 to P5 reacted with the bivalent 2,2'-(ethylendioxy)-diethanthiol in a thiol-ene reaction to form the network, and were simultaneously surface-attached through the C,H-insertion reaction with the benzophenone groups.

crosslinking of polymers P2 to P5, the bifunctional crosslinker 2,2'-(ethylendioxy)-diethanthiol was added to a solution of each polymer in TFE. This polymer-crosslinker solution was then also spin-coated onto benzophenone-functionalized wafer pieces. When UV irradiated, the thiol groups reacted with the double bonds of the poly(oxanorbornene) backbone in a thiol-ene reaction, while the benzophenone groups connected the thus formed polymer network to the substrate (Figure 3b).

The thus obtained polycationic networks P(1-co-Diazo$_{20}$) and P2 to P5 (FTIR spectra shown in Figure S8, Supporting Information) were hydrolyzed to yield the polyzwitterionic networks P(1-co-Diazo$_{20}$)* and P2* to P5* using sodium hydroxide as described by Colak and Tew.[11] Under these conditions, the imide group of the polymers opened, resulting in negatively charged carboxylate functionalities and amide groups carrying positively charged ammonium side chains. To verify the successful hydrolysis, FTIR spectra of the networks before and after hydrolysis were recorded. As an example, **Figure 4** shows the carbonyl region of the spectra of P(1-co-Diazo$_{20}$) (black) and P(1-co-Diazo$_{20}$)* (blue). The polycation had one sharp, high-intensity band at 1706 cm^{-1} which was assigned to the carbonyl of the imide group. After hydrolysis, this band was nearly quantitatively replaced by two new bands at 1658 and 1591 cm^{-1}. These were assigned to the carbonyl groups of the amide and the carboxylate, respectively, which are the expected functional groups in the polyzwitterions. The full spectra of P2–P5 before hydrolysis (Figure S8, Supporting Information), and of P2*–P5* after hydrolysis (Figure S10, Supporting Information) are given in the Supporting Information.

The morphology of the thus obtained polyzwitterionic surfaces was analyzed by atomic force microscopy (AFM) to determine if the substrates were homogeneously covered with polymer. This is crucial because the results of the subsequent physical and biological investigations can only be interpreted correctly if they are not dominated by surface defects. Representative height images of all polymer surface types are shown in **Figure 5**. The root-mean-square (rms) roughness (R_q) of each surface is listed in **Table 2**. The P(1-co-Diazo$_{20}$)* surface was relatively smooth, with an rms roughness of only 0.8 nm. In contrast, the polyzwitterions P2* to P5* that were crosslinked with the low molar mass thiol crosslinker had a porous structure, a consequence of a phase separation between the polymer chains

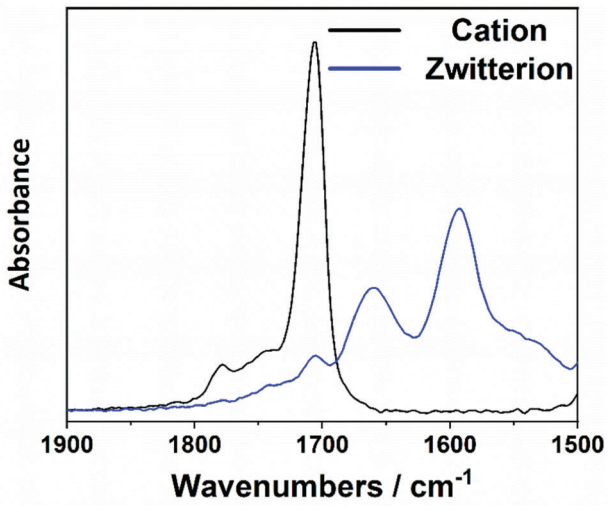

Figure 4. Carbonyl sections from the FTIR spectra of P(1-co-Diazo$_{20}$) (black) and P(1-co-Diazo$_{20}$)* (blue). The band at 1706 cm^{-1} corresponds to the imide group in the cationic network. The bands at 1658 and 1591 cm^{-1} can be assigned to the amide and the carboxylate function of the polyzwitterion, respectively.

and the crosslinker molecules. The rms roughness of these surfaces ranged from 14.5 to 48 nm. Except for these defects, the surfaces were homogenously covered, with an average layer thickness between 192 to 258 nm which was determined by ellipsometry (Table 2). Such porous morphology was reported previously, and it was shown that these defects did not compromise the biological activities of the surfaces as long as the coatings were sufficiently thick.[20–22] Since P(1-co-Diazo$_{20}$)* contained a built-in crosslinker, these surfaces had no marked porosity. Interestingly, the spherical pores became smaller and the rms roughness reduced with increasing alkyl residue length. This could be an indication of improved miscibility of the bivalent thiol crosslinker with the more hydrophobic polymers.

To estimate the hydrophobicity of the polyzwitterionic surfaces, their static, advancing, and receding water contact angles (CAs) were measured (Table 2). For P(1-co-Diazo$_{20}$)*, it was not possible to measure a reproducible contact angle due to its high hydrophilicity. The static CAs of P2*, P3*, and P4* were very similar (32° to 34°) and comparable to static CAs for such polyzwitterions found in the literature.[7,21,22] Changes in the alkyl residue lengths in that range thus did not have a profound impact on the hydrophobicity of the surface. Only P5* showed a significantly higher static contact angle (60°). In the study by Colak and Tew, surfaces covered with the same polymer showed a static contact angle of 70°, which is comparable with the value of this study.[11] The observed difference might be due to the different crosslinking methods used in that work compared to our study.

The swellability in water was used as a second parameter to estimate the hydrophobicity of the surfaces. Swelling data was determined by surface-plasmon resonance spectroscopy (SPR). The data thus obtained are listed in Table 2. The swellability in water decreased with the increasing length of the alkyl residue in the side chain of the polymer, with values between 3.2 and 2.3. Based on the contact angle measurements, one would have expected a drastically lower swellability for P5*. Notably, the swellability data indicate differences between P2* to P4* which are not captured by the contact angle measurements. The absolute swellability values were higher than those reported for polyzwitterionic networks in the literature: for PZI and PCB (Figure 1a), Kurowska et al. reported a swellability of 1.9. In this study, a tetravalent crosslinker was used which might have formed a more densely crosslinked network. A higher number of crosslinks would result in a lower swellability, so the data is not 1:1 comparable, yet the values obtained are in a similar range and thus consistent.

The pH-dependent surface zeta potential of the polyzwitterionic surfaces P(1-co-Diazo$_{20}$)* and P2* to P4* was measured via electrokinetic measurements at different pH values. The titration curves obtained from these measurements are shown in **Figure 6**, the characteristic values (isoelectric Point IEP, ζ_{phys}, pK, ζ_{max}, ζ_{min}) resulting from the measurements are listed in Table 2. All the curves showed a sigmoidal shape of the pH-dependent zeta potential, which is characteristic of pH-responsive polyzwitterionic networks. Expectedly, the zeta potential was positive at low pH and negative at high pH. The IEPs were in the slightly acidic range, and ζ_{phys} was negative. Overall, these results matched those of previously reported pH-responsive polyzwitterions,[21–23] yet some minor differences were also observed. Interestingly, the pK of the acid groups and the maximum zeta potential (ζ_{max}) were similar (within the accuracy of the method) for the polyzwitterionic surfaces with short alkyl residues up to P4* (pK from 3.9 to 4.1; 31 mV < ζ_{max} < 36 mV). Only the surface covered with P5* showed a significantly higher pK of 5.0 and a higher ζ_{max} of 46 mV. The pK of all the polymers was in a range of small molecule carboxylic acids (for example, the pK of acetic acid is 4.76). In literature studies of PCB, the pK of that compound was apparently shifted to lower values, and a second pK value appeared due to side reactions during titration.[20,21] This was not the case for the structures investigated in this study. Looking at the IEP, the values of P2*, P3*, and P4* were also very close (from pH 5.6 to 5.9). In contrast, the IEP of P(1-co-Diazo$_{20}$)* was significantly lower (pH 5.0) and that of IEP of P5* was higher (pH 6.7). The reasons for these deviations are not yet fully understood. They seem to be related to the hydrophobicity of these structures, which will affect the organization of the functional groups at the polymer-liquid interface during titration, and may influence the chemical availability of the functional groups for protonation or neutralization reactions during the measurements.

2.4. Protein Adsorption and Biological Characterization

Polyzwitterionic surfaces are known to resist the adsorption of biological compounds like proteins. In this study, the protein adhesion of the polyzwitterionic networks was investigated with SPR using fibrinogen as a model protein. The aim was to study how the change of the alkyl residue affects the interaction of the polyzwitterionic surface with proteins. To that end, the surfaces were exposed to a solution containing the protein fibrinogen at pH 7.4, and the reflectivity was monitored in situ by SPR kinetics measurements until protein adhesion reached an equilibrium state. Then, the surfaces were washed with buffer solution to remove the reversibly attached protein, and dried. In addition to the kinetics measurements, the amount of irreversibly attached

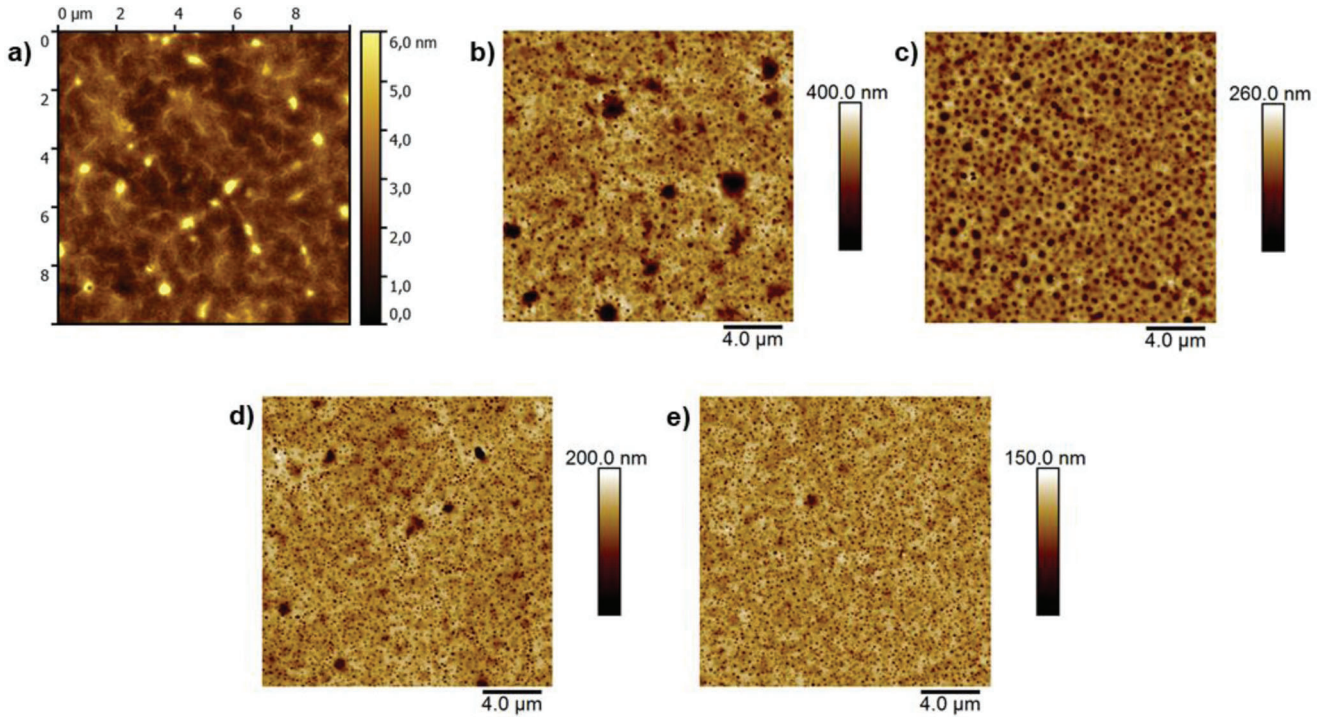

Figure 5. Representative AFM height images of the surface-attached polyzwitterion networks. a) P(1-co-Diazo$_{20}$)*; b) P2*; c) P3*; d) P4*; and e) P5*. P(1-co-Diazo$_{20}$)* shows a very smooth surface compared to the other polymers, which had an overall porous structure.

Table 2. Physical characterization of the surface-attached polyzwitterion networks: layer thickness (determined by ellipsometry); rms roughness (R_q) calculated from the AFM images; static, advancing (adv.) and receding (rec.) water contact angles(CAs); swellability in water (determined by SPR); pH-dependency of the zeta potential obtained from electrokinetic measurements; IEP = isoelectric point (at $\zeta = 0$ mV), $\zeta_{phys} = \zeta$ at pH 7.4; adsorption of fibrinogen (reported as average thickness of the absorbed fibrinogen layer) at pH 7.4.

Polymer	layer thickness [nm]	R_q [nm]	static CA [°]	adv. CA [°]	rec. CA [°]	swell-ability in H_2O	IEP	ζ_{phys} [mV]	pK	ζ_{max} [mV]	ζ_{min} [mV]	protein ads [nm]
P(1-co-Diazo$_{20}$)*	158 ± 3	0.8	< 10	< 10	< 10	n.d.	5.0 ± 0.1	−33 ± 1	4.1 ± 1	36 ± 1	−35 ± 1	0.8 ± 1
P2*	192 ± 1	48.0	32 ± 1	< 10	< 10	3.2 ± 0.2	5.9 ± 0.1	−13 ± 5	4.1 ± 0.2	31 ± 5	−23 ± 5	0.0 ± 1
P3*	202 ± 2	30.9	32 ± 1	< 10	< 10	2.9 ± 0.2	5.6 ± 0.1	−23 ± 5	4.1 ± 0.2	31 ± 5	−33 ± 5	0.0 ± 1
P4*	233 ± 1	21.7	34 ± 1	< 10	< 10	2.7 ± 0.1	5.6 ± 0.1	−24 ± 5	3.9 ± 0.2	36 ± 5	−35 ± 5	0.6 ± 1
P5*	258 ± 1	14.5	60 ± 1	49 ± 1	30 ± 1	2.3 ± 0.3	6.7 ± 0.1	−17 ± 5	5.0 ± 0.2	46 ± 5	−42 ± 5	3.9 ± 1

fibrinogen was quantified by comparing angular reflectivity measurements of the dry substrates taken before and after the kinetics experiment. The results of the SPR experiments (kinetics and the angular reflectivity curves before and after the experiment) for all polymer surfaces are summarized in **Figure 7**, and the amount of irreversibly adhered protein on each surface is given in Table 2. From the kinetics experiments performed with P(1-co-Diazo$_{20}$)*, P2*, P3*, and P4* (Figure 7a–d), it can be seen that these materials absorbed a certain amount of protein, but that this process was almost fully reversible, as the reflectivity value almost reached the baseline after washing with buffer. Also, there was only a small shift of the minimum of the corresponding full reflectivity scans. Fitting this data with simulated curves gave an average layer thickness of the irreversibly adsorbed fibrinogen of < 1 nm. From these results, it could be concluded that networks made from P(1-co-Diazo$_{20}$)*, P2*, P3*, and P4* indeed repelled the adsorption of fibrinogen and thus behaved as expected for polyzwitterionic surfaces. In contrast, P5* adsorbed significant amounts of fibrinogen (average layer thickness: 3.9 nm), and here the adsorption was almost fully irreversible, as hardly any protein was removed after washing with buffer. This result is in good agreement with the result reported by Colak and Tew[10] and matches the results of the water contact angle measurements for this polymer obtained in this study. It indicates a substantially higher hydrophobicity for P5* than for the other polyzwitterionic surfaces. A correlation between protein adsorption and the water contact angle has been reported in the literature.[34] It was stated that protein will adsorb to a surface when the static contact angle of a surface is higher than 60° (the so called Berg-limit),[34] which is near the value found for P5*.

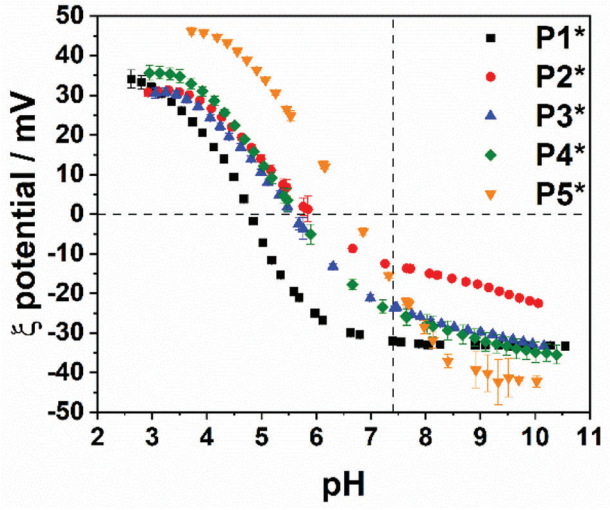

Figure 6. pH-dependent surface zeta potential of the different polyzwitterionic networks obtained by electrokinetic measurements. The horizontal dashed black line marks $\zeta = 0$ mV (i.e., the isoelectric points, IEPs); the vertical dashed black line marks pH 7.4 for estimation of ζ_{phys}.

Recently, it has been reported that certain polyzwitterionic surfaces were intrinsically antimicrobially active.[20–23] pH-responsiveness of the negatively charged group was found to be one key requirement for polyzwitterions to kill bacteria.[22] Yet other pH-responsive polyzwitterions did not show any antimicrobial activity.[15,16,29,30] Since it is known from studies on polycationic antimicrobial networks that their hydrophobicity is important for antimicrobial activity,[31] we assumed that a similar effect would be found for polyzwitterions. Thus, standardized antimicrobial assays were been performed on P(1-co-Diazo$_{20}$)* and P2* to P5* using *Escherichia coli* (*E. coli* ATCC25922) and *Staphylococcus aureus* (*S. aureus* ATCC6538) bacteria. The results of these tests are summarized in **Figure 8**. First, a simplified version of the Japanese Industrial Standard JIS Z 2801 with 5×10^2 bacteria (called screening assay in the following) was used to test the polymer surfaces for general antimicrobial activity. In this screening assay, all the surfaces were tested against *E. coli* bacteria (Figure 8a). After 4 h of incubation, only P5* showed significant activity against this kind of bacteria. On all the other surfaces, bacteria grew as well as on the growth control, or better even better. To get a more quantitative result for the antimicrobial activity of P5*, that material was further tested using a modified version of the JIS-assay with 10^5 colony-forming units (CFUs) of *E. coli* and *S. aureus*. The results are shown in Figure 8b and Figure 8c, respectively. For *E. coli*, no reduction in bacterial growth was observed after 24 h, indicating that the antimicrobial activity of P5* was not sufficient to kill the larger share of bacteria used in this assay. In contrast, there was a two-log reduction in the growth of *S. aureus* on P5* after 24 h. Thus, the P5* surfaces are only mildly antimicrobial and only work well when the bacterial load is not too high, while the other materials are inactive.

The cytocompatibility of the polyzwitterionic surfaces was investigated using human mucosal keratinocytes (for P(1-co-Diazo$_{20}$)*) and human dermal keratinocytes (HaCaT, for P2*, P3*, P4*, and P5*). First, the cells were seeded onto the surfaces and were incubated for up to 48 h at 37 °C. After 24 and 48 h,

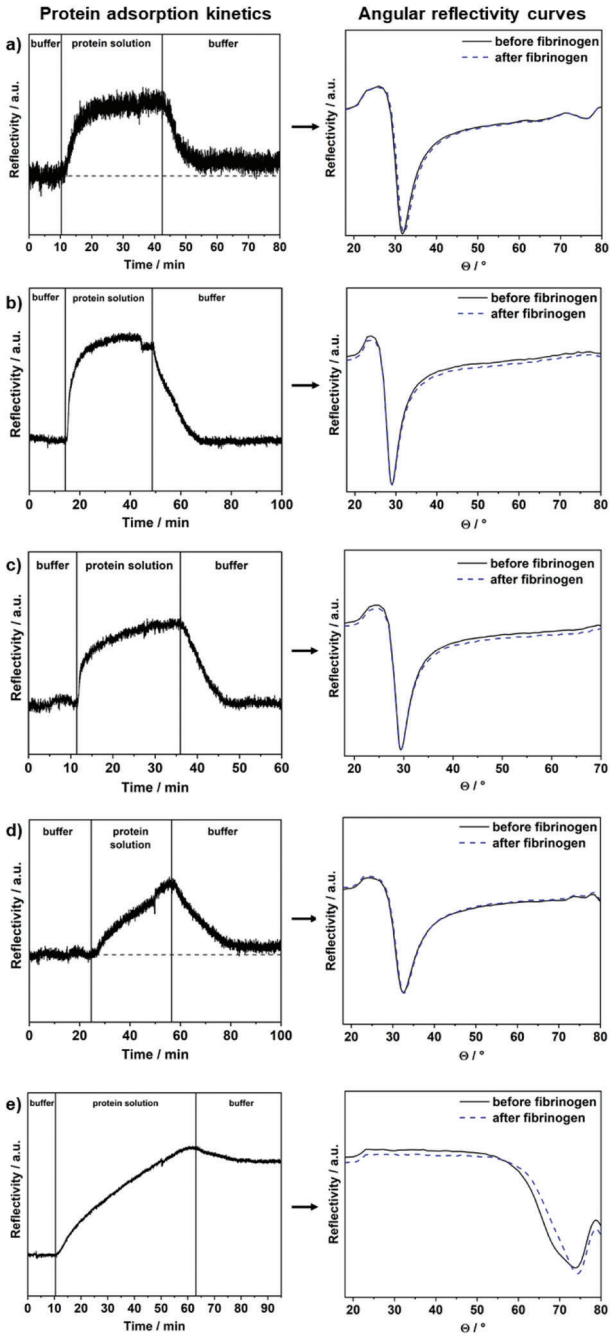

Figure 7. Fibrinogen adhesion on polyzwitterionic surface-attached networks studied by SPR. Left: kinetics measurements, right: full reflectivity scans of the dry materials before and after protein adhesion. a) P(1-co-Diazo$_{20}$)*; b) P2*; c) P3*; d) P4*; and e) P5*. Only P5* adsorbed a substantial amount of fibrinogen.

the cell metabolism was quantified using the Alamar Blue assay (**Figure 9**a, b).

Optical micrographs were also taken at these time points (Figure S11a,b, Supporting Information). For P(1-co-Diazo$_{20}$)*, the dye reduction (which is proportional to the cell metabolism) was as high as on the growth control (a bare glass coverslip), but decreased with longer incubation times. As can be seen

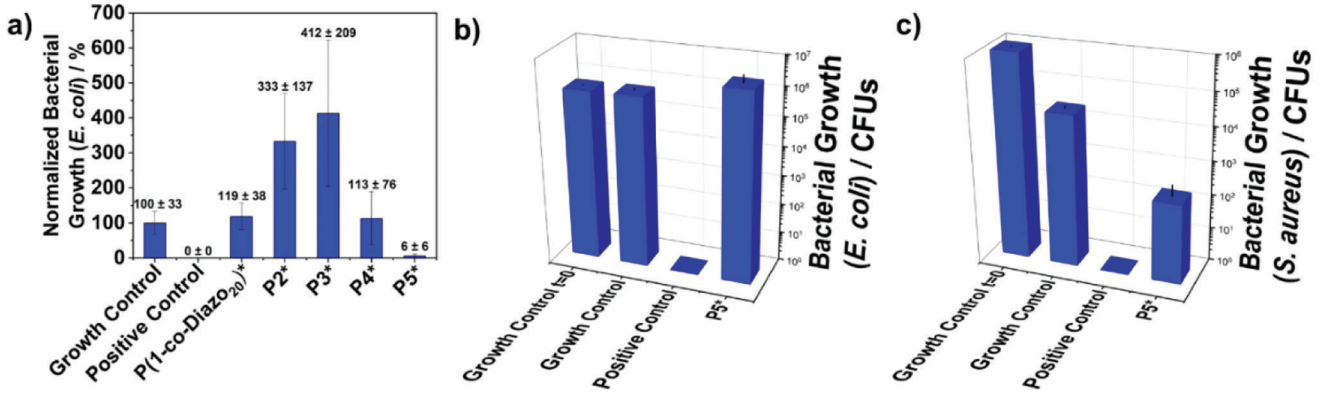

Figure 8. Antimicrobial activity of the polyzwitterionic networks. PZI was used as a positive control in all experiments. a) Normalized growth of *E. coli* in the screening assay; b) growth of *E. coli* on P5* in the JIS-assay; c) growth of *S. aureus* on P5* in the JIS-assay. For the JIS-assays, results from one test replicate are shown here. Data from the additional replicates are shown in Tables S1 and S2, Supporting Information.

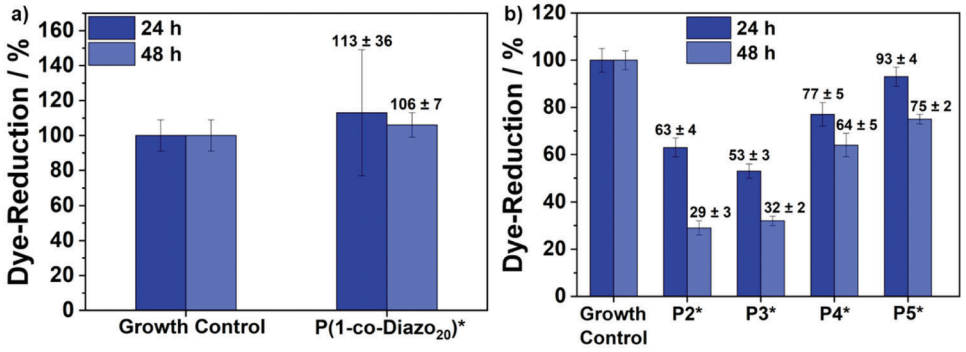

Figure 9. Cell viability on polyzwitterionic networks after 24 and 48 h incubation time determined by the Alamar Blue assay (shown as dye reduction relative to a growth control (uncoated glass coverslips)). a) P(1-co-Diazo$_{20}$)* with gingival mucosa keratinocytes and b) P2*, P3*, P4*, and P5* with HaCaT cells.

in Figure S11a, Supporting Information, the cells were only loosely attached to the surface (as indicated by the round shape of the cells) and the cell density also slightly decreased at longer incubation times. This explains the lower dye reduction at longer incubation times. Thus, unlike most polyzwitterionic surfaces reported in the literature,[12,21,35,36] P(1-co-Diazo$_{20}$)* is not strongly cell-repellant but also does not enable firm cell attachment (which would lead to cell elongation as observed on the growth control). As can be seen in Figure S11b, Supporting Information, the behavior of P2*, P3*, and P4* matched the results of the literature. On these substrates, almost no cells were attached, and if so only loosely (round shape). This explains the low dye reduction amounts of cells grown on these materials (Figure 9b). Still, the surfaces are assumed to be cell compatible as these results hint at a cell adhesion problem, not at cell toxicity. A different behavior was found for the P5* networks. On this material, the cell density increased with longer incubation time and elongated cells were visible after 48 h. At the same time, the dye reduction (Figure 9b) decreased with longer incubation times. Thus, the P5* surface was cell adherent but also slightly toxic to human cells, so that their metabolism was downregulated. The improved adhesion of the cells matches on P5* matches the protein adhesion data, which is also higher on that material than on the other polyzwitterionic materials. As cell adhesion is protein-mediated, these data are consistent and plausible. To the best of our knowledge, this is the first cell-adhesive and cell-toxic polyzwitterionic material so far reported. PZI and PSB, which were also reported to be cell-adherent, showed a good cell viability in the Alamar Blue assay.[20]

3. Conclusion

The aim of this study was to synthesize a set of polyzwitterionic networks with increasing hydrophobicity and to assess the influence of this molecular parameter on their physical properties and bioactivity. The synthesis of these networks was accomplished via polycationic precursor polymers which carried different alkyl residues. These were surface-immobilized and hydrolyzed to yield the polyzwitterionic networks. The physical characterization of these networks showed that the surfaces were smooth when using an internal crosslinker (P(1-co-Diazo$_{20}$)*), and had a porous morphology when using an additional low molecular mass crosslinker. This was in line with previous reports from our group. Water contact angle measurements revealed that all surfaces were strongly hydrophilic, except for the polymer network P5* with the longest alkyl residue. The octyl residue in the polymer side chain of P5* dramatically increased the hydrophobicity of the surface. Surface zeta potential

measurements of the different polyzwitterionic surfaces showed that all polyzwitterionic materials were pH-responsive, as expected for polyzwitterions with a carboxylate group. It was also found that the increased hydrophobicity of P5* had an influence on the protonation/deprotonation-equilibrium, shifting the isoelectric point and the pK of the polymer surface. The hydrophobic character of P5* leads to irreversible adsorption of fibrinogen, while the other more hydrophilic materials repelled proteins, as expected for polyzwitterions. This behavior was reflected in the bioactivity profile of the materials: here, the four more hydrophilic polyzwitterionic networks that resisted protein adhesion were also cell-repulsive. They showed good cell compatibility and were not antimicrobial. In contrast, the hydrophobic P5* surfaces were mildly antimicrobial, and adhesive for human cells, but also showed signs of cell toxicity.

Thus, in this study, it was shown that it is possible to modify the physical properties and bioactivity profile of polyzwitterionic surfaces by modifying their hydrophobicity. This is in good agreement with the well-known fact that proteins can adsorb on hydrophobic surfaces, for example by unfolding and attaching their hydrophobic domains to these materials. The increase of protein adsorption with hydrophobicity was not a linear effect, since increasing the alkyl chains from R = methyl to ethyl, butyl and even hexyl did not alter the property profile much. Instead, there seemed to be a hydrophobicity threshold at R = octyl, at which all physical and biological properties measured experienced a substantial change. It is yet to be determined whether this is a molecular effect or related to the self-organization (e.g., aggregation or crystallization) of the alkyl changes at the polymer-water interfaces. One can assume also that the alkyl chains significantly dilute the zwitterion density at that interface and thereby break the characteristic hydrogen-bond network normally found near polyzwitterionic surfaces.

While the here presented set of polymers could not be optimized to a point where full protein repellency, good cell compatibility, and high antimicrobial activity could be united in a single material, as it was the case for PZI, PCB, IA-PZI, and PNCB, this study confirmed that hydrophobicity is also a determining factor for the overall antimicrobial activity of otherwise similar pH-responsive polyzwitterions in their protonated state. It also showed that the distribution of the hydrophobicity along the polymer chain can be used to tune the cell toxicity—a result that is in line with the findings from the field of Synthetic Mimics of Antimicrobial Peptides.

4. Experimental Section

Materials: All materials used, as well as their commercial sources, are listed in Section S1, Supporting Information.

Instrumentation: NMR spectra were recorded on a Bruker (Billerica, MA, USA) 250 MHz spectrometer using $CDCl_3$, deuterated methanol (CD_3OD), DMSO-d_6, or water (D_2O) as solvent. Gel permeation chromatography (GPC) was performed in trifluoroethanol with 0.05 M potassium trifluoroacetate at 40 °C on a PSS PFG Linear M column (PSS, Mainz, Germany) using a Soma UV/Vis detector at a wavelength of 230 nm. The system was calibrated with poly(methyl methacrylate) standards (PSS, Mainz, Germany). Attenuated total reflection Fourier transform infrared spectra (ATR-FTIR) were recorded on a Cary 630 FTIR Spectrometer (Agilent Technologies, Santa Clara, CA, USA). Transmission FTIR spectra were recorded on a Bio-Rad Excalibur spectrometer (Bio-Rad, München, Germany). For the FTIR measurements, the polymers were immobilized on double-side polished silicon wafers, and a blank wafer was used for background correction. For spin coating of the polymers, a SPIN150 spin coater (SPS-Europe, Putten, Netherlands) was used.

Physical Characterization: The thickness of the dry polymer layers was measured with a SE400adv ellipsometer (Sentech Instruments GmbH, Berlin, Germany). Three measurements on different spots of the sample were taken, and the average was calculated. AFM was used to analyze the surface topography. A Dimension FastScan from Bruker (Billerica, MA, USA) was used with commercial ScanAsyst Air cantilevers (also from Bruker, length 115 µm; width 25 µm; spring constant 0.4 N m^{-1}, resonance frequency 70 kHz). All AFM images were recorded in ScanAsyst Air-mode. The obtained images were analyzed and processed with the Nanoscope Analysis 9.1 software. Zeta potential was measured via electrokinetic surface characterization which was performed on an electrokinetic analyzer with an integrated titration unit (SurPass, AntonPaar GmbH, Graz, Austria). The analyzer was equipped with an adjustable gap cell. Ag/AgCl electrodes were used to detect the streaming current. For these experiments, the polymers were spin-cast on fused silica substrates (20 × 10 × 1 mm, MaTecK, Jülich, Germany) and attached to the substrate holders of the measuring cell. Before each measurement, the electrolyte hoses were rinsed with ultrapure water until a conductivity < 0.06 mS m^{-1} was reached. The measuring cell was then mounted inside the instrument and the electrolyte solution (1 mM KCl) was prepared. The pH of the electrolyte solution was adjusted to pH 10 with 0.1 M NaOH prior to filling the electrolyte hoses. The gap height was adjusted to approximately 105 µm while the system was rinsed for 3 min at 300 mbar. Titration measurement was performed with 0.1 M HCl. The target pressure of the pressure ramp was set to 400 mbar. After titration and before each measurement cycle, the system was rinsed for 3 min at 300 mbar. The pressure program was as follows: target pressure, 400 mbar; maximum time, 20 s; current measurement; two repetitions. Representative titration curves (ζ-potential vs pH) are shown in Figure 6. The isoelectric point (IEP, pH where the zeta potential was zero) was determined from the curve. The p*K* has been estimated graphically from the titration curve as reported previously.[20]

Protein Adsorption: Protein adsorption was studied using SPR. To set up the experiment, an angular scan of the coated substrate under a flow of buffer was performed to detect the plasmon signal minimum. The protein adsorption experiments in the kinetic mode were then carried out at $\Theta_{exp} = \Theta_{min} - 1$ by monitoring the signal intensity at that angle versus time. First, the baseline intensity at that angle against buffer was recorded. The protein solution was then injected (fibrinogen solution at a concentration of 1 mg mL^{-1} in triethanolamine buffer (pH 7.4), flow rate 50 µL h^{-1}). After reaching an equilibrium, buffer was injected to remove any loosely adhering protein. The difference in the reflectivity values before protein injection and after the final buffer wash gives a qualitative estimate of whether the surface was protein adhesive. To quantitatively determine the thickness of the adsorbed protein layer after the kinetics experiment, the surfaces were rinsed with distilled water for 15 min to remove residual salt, and then dried under nitrogen flow. Then, another angular reflectivity curve was measured. The thickness of each layer of the material was calculated by simulations of the reflectivity curves based on the Fresnel equations as described previously.[20]

Antimicrobial Activity: To test the antimicrobial activity of the networks, a modification of the Japanese Industrial Standard JIS Z 2801 was used as published elsewhere.[23] For antimicrobial activity screening, *Escherichia coli* (*E. coli*) (ATCC25922) was used. Approximately 5 × 10^2 bacteria were incubated for 4 h on 1 × 1 cm^2 test samples and controls (five replicates each). They were detached using 0.9% NaCl solution with Tween80. 250 µL of that suspension was spread on CASO agar plates and incubated at 37 °C and 5% CO_2 for 18 to 24 h. The colony-forming units (CFUs) were counted after incubation and reported as percent growth relative to the growth control. The antimicrobial activity of polymer networks that were found to be highly active in the screening assay was confirmed using a modified JIS assay with 10^6 CFUs with either *E. coli* or *S. aureus* (*S. aureus* ATCC6538). Key changes in this assay compared to the original protocol of the Japanese Industrial Standard JIS Z 2801 were the reduction

Table 3. Reagent and solvent amounts (monomer, comonomer (only for P(1-co-Diazo$_{20}$)), Grubbs 3rd, TFE, and DCM) used in each of the polymerization reactions.

Polymer	Monomer	Diazo-M	Grubbs 3rd	TFE	DCM
P(1-co-Diazo$_{20}$)	300 mg; 0.83 mmol; 62 eq.	100 mg; 0.30 mmol; 23.0 eq.	9.7 mg; 0.013 mmol; 1 eq.	2.25 mL	2.25 mL
P2	500 mg; 1.27 mmol; 76 eq.	-	12.1 mg; 0.017 mmol; 1 eq.	2.5 mL	2.5 mL
P3	500 mg; 1.19 mmol; 71 eq.	-	12.2 mg; 0.017 mmol; 1 eq.	2.5 mL	2.5 mL
P4	100 mg; 0.25 mmol; 75 eq.	-	2.4 mg; 0.003 mmol; 1 eq.	0.5 mL	0.5 mL
P5	100 mg; 0.23 mmol; 70 eq.	-	2.4 mg; 0.003 mmol; 1 eq.	0.5 mL	0.5 mL

of the sample size to 2.5 × 2.5 cm^2 and a corresponding reduced volume of the bacterial suspension to 100 µL (containing about 1 × 10^6 CFUs). The CFUs were determined after 0 and 24 ± 1 h and were reported as log reduction relative to the negative control.

Cell Viability: Two different but comparable keratinocyte cell lines, human dermal keratinocytes (HaCaT, CLS, Eppelheim, Germany) and human mucosal keratinocytes were used to test the cell compatibility. HaCaT were cultured in Dulbecco's Modified Eagle's Medium (DMEM) supplemented with 4.5 g L^{-1} glucose, 2 mM L-glutamine, and 10% fetal calf serum (FCS). At a cell confluence of 80–90%, the cells were detached with TrypLETM express (life technologies, Darmstadt, Germany). 1 × 10^5 cells were seeded on round glass coverslips (15 mm in diameter; thickness No. 2; ORSAtec, Bobingen, Germany) and incubated in FCS-free DMEM at 37 °C/5% CO_2 to allow the cells to settle. After 4 h, 50% of the medium was discarded and replaced with DMEM at double FCS concentration, yielding a normal FCS concentration in the well for further cultivation (24 and 48 h). Gingival mucosal keratinocytes were cultivated in keratinocyte growth medium (PromoCell, Heidelberg, Germany) supplemented with bovine pituitary extract 0.004 mg mL^{-1}, epidermal growth factor 0.125 ng mL^{-1}, insulin 5 µg mL^{-1}, hydrocortisone 0.33 µg mL^{-1}, epinephrine 0.39 µg mL^{-1}, transferrin 10 µg mL^{-1}, and 60 µg mL^{-1} $CaCl_2$. For detachment, Accutase (Merck, Darmstadt, Germany) was used. After incubating the cells in supplement-free medium, a double concentration of supplements in the medium was used here, too.

The Alamar Blue assay was performed and analyzed according to the manufacturer's protocol (Biorad, Feldkirchen, Germany). For this, 500 µL growth medium was removed and replaced with fresh 500 µL DMEM with FCS containing 10% Alamar Blue solution. The cells were then incubated under physiological conditions for at least 2 h. The plates were centrifuged at 300 g for 5 min, the supernatant was pipetted into another well plate, and the fluorescence intensity was measured (excitation at 540 nm; measurement at 590 nm) using the microplate reader Infinite F Nano Plus (Tecan, Crailsheim, Germany). Within one experiment, technical triplicates were generated for all samples and controls. The experiment was repeated twice. Optical images were obtained using a Primovert Microscope (Zeiss, Oberkochen, Germany) and processed using the ZEN blue software (Zeiss, Oberkochen, Germany).

Synthesis of 2-(2-(dimethylamino)-ethyl)-3a,4,7,7a-tetrahydro-1H-4,7-epoxyisoindole-1,3(2H)-dione (A): The same precursor-structure A was used for all monomers. It was synthesized according to a literature procedure.[37] A suspension of *exo*-3,6-epoxy-1,2,3,6-tetrahydrophthalicanhydride (5 g, 30 mmol) in MeOH (150 mL) was cooled in an ice-bath. A solution of *N,N*-dimethylethylendiamine (2.65 g, 30 mmol, 1 eq) in MeOH (30 mL) was added dropwise. Afterwards, the solution was stirred at room temperature for 1 h and under reflux for another 3 h. The solvent was removed under reduced pressure. The crude was recrystallized from EtOH and dried.

^{1}H-NMR (250 MHz, $CDCl_3$): δ = 2.23 (s, 6H, CH_3), 2.44 (t, J = 6.8 Hz, 2H, N–CH_2), 2.83 (s, 2H, (C=O)–CH), 3.56 (t, J = 6.8 Hz, 2H, (C=O)–N–CH_2), 5.22 (s, 2H, O–CH), and 6.48 (s, 2H, C=CH) ppm.

Synthesis of Methyl Monomer (M1): The compound was synthesized according to a literature procedure.[10] A solution of A (1.00 g, 4.23 mmol) in THF (anhydrous, 10 mL) was cooled in an ice-bath. Dimethylsulfate (0.56 mL, 0.75 g, 5.91 mmol, 1.4 eq) was added dropwise. The mixture was stirred at room temperature for 4 h. Afterwards, the white precipitate was filtered, washed with THF and *n*-hexane and dried.

^{1}H-NMR (250 MHz, D_2O): δ = 3.15 (s, 2H, (C=O)–CH), 3.16 (s, 9H, CH_3), 3.55 (t, 2H, N–CH_2), 3.71 (s, 3H, CH_3SO_4), 3.97 (t, 2H, (C=O)–N–CH_2), 5.32 (s, 2H, O–CH), 6.60 (s, 2H, C=CH) ppm.

Synthesis of Ethyl to Octyl Monomers (M2–M5): All the compounds were synthesized analogously to M1. A solution of precursor **A** (1.00 g, 4.23 mmol) in THF (anhydrous, 10 mL) was heated to 50 °C. The respective alkyl iodide or bromide (1.5 eq) was added and the mixture was stirred for 48 h at 50 °C. After cooling to room temperature, the precipitate was filtered, washed with THF, and dried.

^{1}H-NMR (250 MHz, MeOD): M2: δ = 1.39 (t, 3H, C–CH_3), 3.02 (s, 2H, (C=O)–CH) 3.14 (s, 6H, N–CH_3), 3.40–3.60 (m, 4H, N–CH_2), 3.93 (t, 2H, (C=O)–N–CH_2), 5.20 (s, 2H, O–CH), and 6.58 (s, 2H, C=CH) ppm; M3: δ = 1.03 (t, 3H, C–CH_3), 1.33–1.52 (m, 2H, CH_3–CH_2), 1.67–1.87 (m, 2H, N–CH_2–CH_2), 3.02 (s, 2H, (C=O)–CH), 3.15 (s, 6H, N–CH_3), 3.33–3.45 (m, 2H, N–CH_2–C_3H_7), 3.52 (t, 2H, N–CH_2), 3.93 (t, 2H, (C=O)–N–CH_2), 5.20 (s, 2H, O–CH), and 6.57 (s, 2H, C=CH) ppm. M4: δ = 0.97 (t, 3H, C–CH_3), 1.33–1.52 (m, 6H, CH_3–C_3H_6), 1.72–1.93 (m, 2H, N–CH_2–CH_2), 3.04 (s, 2H, (C=O)–CH), 3.17 (s, 6H, N–CH_3), 3.36–3.46 (m, 2H, N–CH_2–C_5H_{11}), 3.54 (t, 2H, N–CH_2), 3.95 (t, 2H, (C=O)–N–CH_2), 5.22 (s, 2H, O–CH), and 6.60 (s, 2H, C=CH) ppm. M5: δ = 0.94 (t, 3H, C–CH_3), 1.25–1.54 (m, 10H, CH_3–C_5H_{10}), 1.72–1.94 (m, 2H, N–CH_2–CH_2), 3.04 (s, 2H, (C=O)–CH), 3.16 (s, 6H, N–CH_3), 3.36–3.45 (m, 2H, N–CH_2–C_7H_{15}), 3.53 (t, 2H, N–CH_2), 3.95 (t, 2H, (C=O)–N–CH_2), 5.22 (s, 2H, O–CH), and 6.60 (s, 2H, C=CH) ppm.

Polymerization of P2–P5: All polymers P2 to P5 were synthesized following a procedure described in the literature.[38] In each case, the cationic monomer was dissolved in TFE (dried, distilled, and degassed). The Grubbs 3rd generation catalyst was dissolved in DCM (dried and distilled) in a separate vial. The catalyst solution was added to the monomer solution in one shot with an overall ratio TFE:DCM of 1:1 (v/v). After stirring the mixture for 1 h at room temperature, an excess of ethylvinyl ether (1 mL) was added to stop the reaction. The mixture was stirred at room-temperature for another 30 min and the solvents were removed under reduced pressure. The crude product was redissolved in TFE and precipitated from diethyl ether.

Polymerization of P(1-co-Diazo$_{20}$): To obtain P(1-co-Diazo$_{20}$), M1 was copolymerized with Diazo-M (Figure 2b) which had been obtained as described in the literature.[33] Since the latter monomer was not soluble in TFE, it was dissolved in DCM (dried and distilled) separately and added to the solution containing the cationic monomer before adding the catalyst. Other than that, the polymerization and work-up procedure was the same as for polymers P2 to P5 (**Table 3**).

^{1}H-NMR (250 MHz, D_2O): P(1-co-Diazo$_{20}$): δ = 3.17 (br.s., 9H, CH_3), 3.43–3.58 (m, 2H, N–CH_2), 3.58–3.74 (m, 5H, (C=O)–CH, CH_3SO_4), 3.84–4.09 (m, 2H, (C=O)–N–CH_2), 4.63 (br.s., 1H, O–CH), 5.00 (br.s., 1H, O–CH), 5.89 (br.s., 1H, C=CH cis), and 6.09 (br.s., 1H, C=CH trans) ppm. P2: δ = 1.25–1.45 (m, 3H, C–CH_3), 3.13 (br.s., 6H, N–CH_3), 3.36–3.73 (m, 6H, (C=O)–CH, N–CH_2), 3.82–4.07 (m, 2H, (C=O)–N–CH_2), 4.60–4.80 (m, *H*OD, O–CH), 5.15 (br.s., 1H, O–CH), 5.91 (br.s., 1H, C=CH cis), and 6.11 (br.s., 1H, C=CH trans) ppm. P3: δ = 0.95–1.11 (m, 3H, C–CH_3), 1.36–1.57 (m, 2H, CH_3–CH_2), 1.70–1.91 (m, 2H, N–CH_2–CH_2), 3.22 (br.s., 6H, N–CH_3), 3.36–3.79 (m, 6H, (C=O)–CH, N–CH_2), 3.84–

Table 4. Parameters for preparation of the spin-coating solutions.

Polymer	m (Polymer) [mg]	V (Solution A) [mL]	V (TFE)[a)] [mL]	V (TFE)[b)] [mL]
P2	30.0	0.42	0.58	1.08
P3	30.1	0.39	0.61	1.11
P4	30.1	0.41	0.59	1.09
P5	30.0	0.38	0.62	1.12

[a)] Volume of TFE when spin coating onto all substrates except gold. [b)] Volume of TFE when spin coating onto gold.

4.10 (m, 2H, (C=O)–N–CH_2), 4.65–4.85 (m, *H*OD, O–CH), 5.21 (br.s., 1H, O–CH), 5.98 (br.s., 1H, C=CH cis), and 6.17 (br.s., 1H, C=CH trans) ppm.

Polymerization of P4: δ = 0.85–1.01 (m, 3H, C–CH_3), 1.26–1.52 (m, 6H, CH_3–C_3H_6), 1.70–1.95 (m, 2H, N–CH_2–CH_2), 3.19 (br.s., 6H, N–CH_3), 3.31–3.80 (m, 6H, (C=O)–CH, N–CH_2), 3.89–4.12 (m, 2H, (C=O)–N–CH_2), 4.57–4.86 (m, *H*OD, O–CH), 5.13 (br.s., 1H, O–CH), 5.95 (br.s., 1H, C=CH cis), and 6.16 (br.s., 1H, C=CH trans) ppm. P5: δ = 0.78–1.00 (m, 3H, C–CH_3), 1.18–1.52 (m, 10H, CH_3–C_5H_{10}), 1.70–1.96 (m, 2H, N–CH_2–CH_2), 3.25 (br.s., 6H, N–CH_3), 3.39–3.76 (m, 6H, (C=O)–CH, N–CH_2), 3.76- 4.09 (m, 2H, (C=O)–N–CH_2), 4.57–4.94 (m, *H*OMe, O–CH), 5.14 (br.s., 1H, O–CH), 5.89 (br.s., 1H, C=CH cis), and 6.11 (br.s., 1H, C=CH trans) ppm.

Pre-Functionalization of Substrates for Preparation of Polyzwitterionic Surfaces P(1-co-Diazo$_{20}$) and P2* to P5**: For covalent attachment of the polymer networks, the substrates were functionalized with benzophenone anchor groups prior to usage. The molecules used (triethoxy-functionalized benzophenone (3EBP) for all surfaces except gold, lipoic acid-functionalized benzophenone (LS-BP) for gold surfaces) were synthesized after literature procedures.[25,39] Surface functionalization was achieved as described previously.[20]

*Preparation of Polyzwitterionic Surface P(1-co-Diazo$_{20}$)**: The cationic precursor copolymer P(1-co-Diazo$_{20}$) was dissolved in TFE at a concentration of 15 (coating gold substrates) or 30 mg mL^{-1} (for all other substrates) and spin-coated on the respective substrates using the following process parameters: spin speed 3000 rpm, acceleration 1000 rpm s^{-1}, and 30 s spinning time. The coated substrates were crosslinked using UV light at a wavelength of 254 nm with an energy dose of 0.3 J cm^{-2}. Hydrolysis of the imide ring was achieved by immersion of the substrates into aqueous $NaHCO_3$–solution (sat.) overnight. The surfaces were rinsed with demineralized water and dried in a stream of nitrogen.

Preparation of Polyzwitterionic Surface P2 to P5**: A stock solution of 2,2'-(ethylendioxy)-diethanthiol (Solution A, 50 mg mL^{-1} in TFE) was prepared. The spin-coating solutions containing the cationic precursor homopolymers and the crosslinker in TFE were prepared by dissolving 30 mg of each polymer in Solution A and TFE, according to **Table 4**. This way, a molar ratio of double bonds to thiol of 1:3 was achieved for every polymer solution. Spin-coating was used with the following process parameters: spin speed 3000 rpm, acceleration 500 rpm s^{-1}, and 20 s spinning time. The coated substrates were crosslinked using UV light at a wavelength of 254 nm with an energy-dose of 4 J cm^{-2}. Hydrolysis of the imide ring was achieved by immersion of the substrates into an aqueous NaOH-solution (0.1 M) for 20 min. The surfaces were rinsed with demineralized water and dried in a stream of nitrogen.

Supporting Information

Supporting Information is available from the Wiley Online Library or from the author.

Acknowledgements

Funding for this work from the Bundesministerium für Bildung und Forschung (German Ministry for Education and Research, BMBF; VIP+ technology transfer program under the grant acronym ANTIBUG) and from the Deutsche Forschungsgemeinschaft (German Research Foundation, DFG; Heisenberg program, Grant ID LI 1714/9-1) were gratefully acknowledged. The authors thank Sibylle Rau for performing the cell biological experiments with the dermal keratinocytes.

Open Access funding enabled and organized by Projekt DEAL.

Conflict of Interest

The authors declare no conflict of interest.

Data Availability Statement

The data that support the findings of this study are available in the supplementary material of this article.

Keywords

antimicrobial polymers, polyelectrolytes, polyzwitterions, protein-repellent polymers

Received: September 20, 2022
Revised: October 7, 2022
Published online: December 4, 2022

[1] S. Chen, L. Li, C. Zhao, J. Zheng, *Polymer* **2010**, *51*, 5283.
[2] B. Cao, Q. Tang, G. Cheng, *J. Biomater. Sci., Polym. Ed.* **2014**, *25*, 1502.
[3] S. Jiang, Z. Cao, *Adv. Mater.* **2010**, *22*, 920.
[4] S. Kudaibergenov, W. Jaeger, A. Laschewsky, *Adv. Polym. Sci.* **2006**, *201*, 157.
[5] A. Laschewsky, *Polymers* **2014**, *6*, 1544.
[6] E. Schönemann, A. Laschewsky, E. Wischerhoff, J. Koc, A. Rosenhahn, *Polymers* **2019**, *11*, 1014.
[7] J. Koc, E. Schönemann, A. Amuthalingam, J. Clarke, J. A. Finlay, A. S. Clare, A. Laschewsky, A. Rosenhahn, *Langmuir* **2018**, *35*, 1552.
[8] Z. Zhang, T. Chao, S. Chen, S. Jiang, *Langmuir* **2006**, *22*, 10072.
[9] G. Cheng, G. Li, H. Xue, S. Chen, J. D. Bryers, S. Jiang, *Biomaterials* **2009**, *30*, 5234.
[10] S. Colak, G. N. Tew, *Langmuir* **2012**, *28*, 666.
[11] S. Colak, G. N. Tew, *Biomacromolecules* **2012**, *13*, 1233.
[12] B. Li, P. Jain, J. Ma, J. K. Smith, Z. Yuan, H. - C. Hung, Y. He, X. Lin, K. Wu, J. Pfaendtner, S. Jiang, *Sci. Adv.* **2019**, *5*, eaaw9562.
[13] J. B. Schlenoff, *Langmuir* **2014**, *30*, 9625.
[14] C. Leng, S. Sun, K. Zhang, S. Jiang, Z. Chen, *Acta Biomater.* **2016**, *40*, 6.
[15] G. Cheng, H. Xue, Z. Zhang, S. Chen, S. Jiang, *Angew. Chem., Int. Ed.* **2008**, *47*, 8831.
[16] Z. Cao, L. Mi, J. Mendiola, J. - R. Ella-Menye, L. Zhang, H. Xue, S. Jiang, *Angew. Chem., Int. Ed.* **2012**, *51*, 2602.
[17] J. Wang, J. Wei, *Appl. Surf. Sci.* **2016**, *382*, 202.
[18] D. W. Grainger, *Nat. Biotechnol.* **2013**, *31*, 507.
[19] L. Zhang, Z. Cao, T. Bai, L. Carr, J. - R. Ella-Menye, C. Irvin, B. D. Ratner, S. Jiang, *Nat. Biotechnol.* **2013**, *31*, 553.
[20] M. Kurowska, A. Eickenscheidt, D. - L. Guevara-Solarte, V. T. Widyaya, F. Marx, A. Al-Ahmad, K. Lienkamp, *Biomacromolecules* **2017**, *18*, 1373.
[21] M. Kurowska, A. Eickenscheidt, A. Al-Ahmad, K. Lienkamp, *ACS Appl. Bio Mater.* **2018**, *1*, 613.
[22] S. Paschke, R. Prediger, V. Lavaux, A. Eickenscheidt, K. Lienkamp, *Macromol. Rapid Commun.* **2021**, *42*, 2100051.

[23] A. Schneider-Chaabane, V. Bleicher, S. Rau, A. Al-Ahmad, K. Lienkamp, *ACS Appl. Mater. Interfaces* **2020**, *12*, 21242.
[24] W. Hartleb, J. S. Saar, P. Zou, K. Lienkamp, *Macromol. Chem. Phys.* **2016**, *217*, 225.
[25] P. Zou, W. Hartleb, K. Lienkamp, *J. Mater. Chem. A* **2012**, *22*, 19579.
[26] S. M. Elsayed, V. T. Widyaya, Y. Shafi, A. Eickenscheidt, K. Lienkamp, *Molecules* **2019**, *24*, 3371.
[27] V. T. Widyaya, C. Müller, A. Al-Ahmad, K. Lienkamp, *Langmuir* **2019**, *35*, 1211.
[28] L. Mi, S. Jiang, *Angew. Chem., Int. Ed.* **2014**, *53*, 1746.
[29] P. Sobolčiak, M. Špírek, J. Katrlík, P. Gemeiner, I. Lacík, P. Kasák, *Macromol. Rapid Commun.* **2013**, *34*, 635.
[30] B. Cao, Q. Tang, L. Li, J. Humble, H. Wu, L. Liu, G. Cheng, *Adv. Healthcare Mater.* **2013**, *2*, 1096.
[31] P. Zou, D. Laird, E. K. Riga, Z. Deng, F. Dorner, H. - R. Perez-Hernandez, D. L. Guevara-Solarte, T. Steinberg, A. Al-Ahmad, K. Lienkamp, *J. Mater. Chem. B* **2015**, *3*, 6224.
[32] A. Himmelsbach, A. Schneider-Chaabane, K. Lienkamp, *Macromol. Chem. Phys.* **2019**, *220*, 1900346.
[33] E. K. Riga, J. Rühe, K. Lienkamp, *Macromol. Chem. Phys.* **2018**, *219*, 1800397.
[34] E. Schönemann, J. Koc, N. Aldred, A. S. Clare, A. Laschewsky, A. Rosenhahn, E. Wischerhoff, *Macromol. Rapid Commun.* **2020**, *41*, 1900447.
[35] Z. Zhang, S. Chen, Y. Chang, S. Jiang, *J. Phys. Chem. B* **2006**, *110*, 10799.
[36] W. Yang, H. Xue, L. R. Carr, J. Wang, S. Jiang, *Biosens. Bioelectron.* **2011**, *26*, 2454.
[37] R. Auvergne, R. Saint-Loup, C. Joly-Duhamel, J. J. Robin, B. Boutevin, *J. Polym. Sci., Part A: Polym. Chem.* **2007**, *45*, 1324.
[38] D. A. Rankin, A. B. Lowe, *Macromolecules* **2008**, *41*, 614.
[39] M. Gianneli, R. F. Roskamp, U. Jonas, B. Loppinet, G. Fytas, W. Knoll, *Soft Matter* **2008**, *4*, 1443.

